Global Land Cover Mapping – Need for Discrete Global Grid System

Frane Gilić[1,], Martina Baučić[1], Samah Termos[2]*

[1] Faculty of Civil Engineering, Architecture and Geodesy, University of Split, Split, Croatia, fgilic@gradst.hr, mbaucic@gradst.hr
[2] Remote Sensing Center, Lebanese National Council for Scientific Research, Beirut, Lebanon, samahtermos@gmail.com
* corresponding author
doi: 10.5281/zenodo.11621508

Abstract: The quality of land cover maps is gradually advancing in terms of increased spatial and temporal resolution, and classification accuracy. However, the aspect of spatial referencing and techniques for representing land cover data has not been advancing. Representing land cover data in the form of a planar raster geospatial data model is still common, despite the various issues especially evident when working with global land cover data. This paper first analyses current approaches in georeferencing global LCLU datasets. Then it examines differences in areal calculations from raster data georeferenced in projected and geographic coordinate reference systems (CRSs). This analysis is performed for the case study of calculating built-up land cover change for the Lebanese 10-km coastal zone. Finally, this paper introduces the topic of discrete global grid systems (DGGSs) as a relatively new approach to handling global geospatial data. DGGSs manage spatial data on the surface of the ellipsoid, rather than in the flattened raster model and thus represent a step forward in managing global geospatial data.

Keywords: land cover; land use; raster; map projection; DGGS.

1 Introduction

Satellite images and the development of methods for their automatic analysis made possible producing land cover / land use (LCLU) data covering large areas, even the whole surface of the Earth. These kinds of satellite-images-derived LCLU products are almost exclusively delivered in a raster data format (Table 1) which is the reason why the analysis in this paper is limited only to the raster datasets. Well known problem that is related to handling geospatial data that cover large areas is the problem of distance, shape and area distortions associated with the traditional approach of flattening data from the Earth's surface. In the case of LCLU data, this flattening is usually performed by equal-area map projections.

The study elaborated by Steinwand et al. (1995) has identified the equal-area projections with the smallest distortions for raster data. In addition to distortions due to map projection, the authors analysed pixel distortion caused by reprojection. The study identified the interrupted Goode Homolosine, the interrupted Mollweide, the Wagner IV and Wagner VII as the best for global maps, the Lambert Azimuthal Equal-Area for hemispheric maps, and the oblated Equal-Area and the Lambert Azimuthal Equal-Area for continental maps. The interrupted map projections introduce computational issues and are not fully supported by today's software (Moreira de Sousa et al. 2019). However, by examining recent global LCLU products, the trend is to georeference global LCLU datasets in geographic coordinate reference systems (CRSs), rather than in projected ones. This can be observed from the data in Table 1 which lists some technical characteristics of five notable recent global LCLU products: ESA WorldCover (Zanaga et al. 2021), Esri's Sentinel-2 LCLU (Karra et al. 2021), GLC_FCS30D (Zhang et al. 2024), Dynamic World (Brown et al. 2022), and GLAD (Global Land Analysis and Discovery laboratory) LCLU dataset (Potapov et al. 2022). Visualisations of these LCLU datasets over the Lebanese capital Beirut are shown in Figure 1.

Georeferencing raster LCLU datasets in geographic CRS imposes various issues, including data replication due to meridian convergence (Figure 2a). This issue can be solved by keeping angular pixel size constant in a north-south direction and defining latitudinal zones with varying pixel sizes in an east-west direction (e.g., Defence Gridded Elevation Data standard (DGED, DGIWG 2020)). Another issue is related to performing areal calculations, which, although possible in modern GIS applications, is more complex in geographic CRSs than in projected ones. From the LCLU point of view, a particularly interesting class of DGGSs are equal-area ones that have cells with the same area on the same refinement level (i.e., hierarchical level).

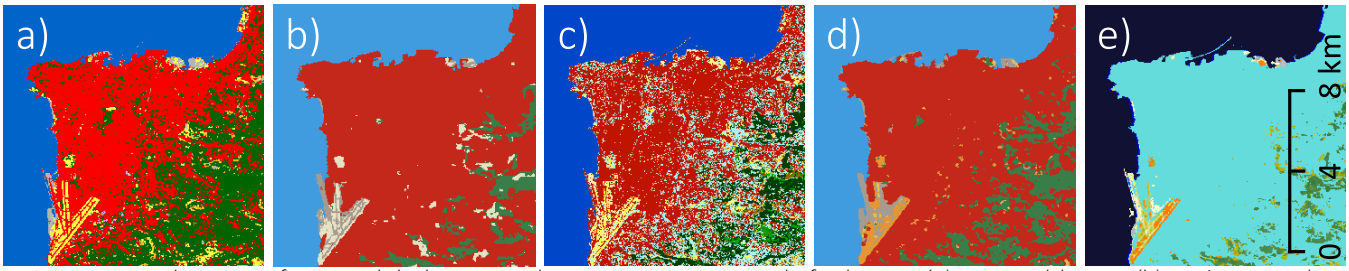

Figure 1. Visualizations of recent global LCLU products over Beirut, capital of Lebanon: (a) ESA WorldCover, (b) Esri's Sentinel-2 LCLU, (c) GLC_FCS30D, (d) Dynamic World, and (e) GLAD LCLU.

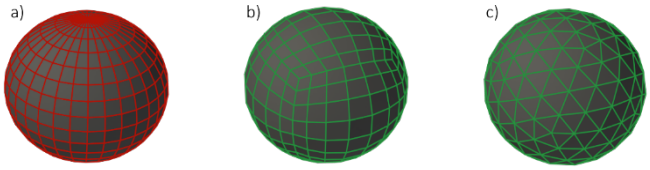

Figure 2. Discretisation of the surface of the ellipsoid by (a) grid of meridians and parallels and discrete global grid with (b) quadrangle cells and (c) triangle cells.

Table 1. Data format, CRS, and pixel size of recent global LCLU products.

LCLU product	Data format	CRS	Pixel size
ESA WorldCover	Raster, GeoTIFF (unsigned 8-bit integer, DEFLATE compression)	Geographic, WGS 84 (EPSG:4326)	0.30" (≈ 9.3 m at the equato)
Esri's Sentinel-2 LCLU	Raster, GeoTIFF (unsigned 8-bit integer, LZW compression)	Projected, WGS 84 / UTM	10.0 m
GLC_FCS30D	Raster, GeoTIFF (unsigned 8-bit integer, LZW compression)	Geographic, WGS 84 (EPSG:4326)	0.97" (≈ 30.0 m at the equator)
Dynamic World*	Raster, GeoTIFF (unsigned 8-bit integer, LZW compression)	Geographic, WGS 84 (EPSG:4326)	0.32" (≈ 10.0 m at the equator)
GLAD LCLU	Raster, GeoTIFF (unsigned 8-bit integer, LZW compression)	Geographic, WGS 84 (EPSG:4326)	0.90" (≈ 27.8 m at the equator)

*listed data correspond to the default download options on the Google Earth Engine.

Therefore, DGGSs solve the problem of distortions imposed by map projections by directly discretizing the surface of the ellipsoid (Figure 2b and 2c) and equal-area ones simplify the problem of areal calculations on the surface of the ellipsoid. DGGS can be viewed as a way of georeferencing spatial data, instead of using coordinates, and as a geospatial data format, along with vector and raster models (Kmoch et al. 2022). Differences between DGGS and traditional (i.e., flattened) GIS approaches are provided by Li and Stefanakis (2020).

In this paper we examine differences in calculation procedures and obtained results from calculating change in an area of built-up land cover class from LCLU data georeferenced in projected and in geographic CRS. We also discuss what would be the benefits of referencing LCLU data with DGGSs.

2 Materials and methods

To illustrate the difference in processing procedure and obtained results when working with data georeferenced in the geographic and in projected CRSs, we decided to calculate the change in built-up area from 2015 to 2020 for the Lebanese 10-km coastal zone (i.e., zone that is 10 km inland from the coastline, hereafter 10-km CZ). We have chosen the GLC_FCS30D LCLU product for this calculation, which, as can be seen from Table 1, is delivered as a raster dataset georeferenced in the WGS 84 geographic CRS. Pixels are 0.97" wide in latitude and longitude direction. For the Lebanese 10-km CZ, which approximately spans from a latitude of 33°05' N to 34°39' N (WGS 84), GLC_FCS30D pixel sizes in east-west direction range from 25.2 to 24.7 m. In the north-south direction, pixel sizes are more stable, ranging from 29.8 m at the equator to 30.1 m at the poles. Along with GLC_FCS30D, we used the coastline and administrative border of Lebanon to construct a 10-km CZ which we afterwards spatially intersected with the Lebanese governorates. Those data were exported from the OpenStreetMap vector data and are also georeferenced in WGS 84 geographic CRS. All calculations were performed in the QGIS (version 3.28.6) free and open-source GIS application (with GDAL library version 3.6.4 and GRASS GIS provider plugin version 2.12.99).

2.1 Calculating area in projected CRS

When there is a task to compute areal statistics from data georeferenced in geographic CRS, the traditional approach would be to first convert data from geographic CRS to projected CRS that is based on the equal-area map projection or projection that introduces a tolerable level of areal distortions. After this conversion, the area is calculated by simply counting the number of desired pixels and then multiplying it with the constant area of each pixel. However, the problem with this approach is that it requires reprojecting the LCLU raster dataset, which inevitably introduces data loss (Lu et al. 2018). In this research, we decided to reproject the GLC_FCS30D LCLU raster to the projected Universal Transverse Mercator (UTM) zone 36N CRS (EPSG: 32636) with target pixel sizes of 25x30 m. UTM is not an equal-area projection but for most applications level of deformations it introduces is negligible. Calculating area, in this case, is straightforward: with the *Zonal statistics* tool in QGIS, it is possible to count the number of pixels corresponding to the built-up class in each governorate within a 10-km CZ and then multiply it with 750 m^2 (25x30 m^2) for 2015 and 2020.

2.2 Calculating area in geographic CRS

Another approach is to keep GLC_FCS30D data in geographic CRS. Pixels in this case are quadrangles bounded by meridians and parallels and it is possible to determine their area with a direct formula (Lapaine and Lapaine 1991). GRASS GIS provider, which is a QGIS plugin, enables using tools from the GRASS GIS application. One such tool is a *r.mapcalc.simple* tool that implements an *area()* expression. This expression enables generating a new raster in which pixel values correspond to the area of each GLC_FCS30D pixel on the surface of the ellipsoid. Then, with a common *Raster calculator* tool in QGIS, it is needed to generate a new raster with extracted pixels that correspond to the built-up class for each year. Finally, to calculate the final built-up areas, a *Zonal statistics* tool is required to summarize pixel values (i.e., their areas) within each Lebanese governorate.

3 Results

Table 2 lists areas of built-up land cover class calculated from GLC_FCS30D raster data georeferenced in WGS 84 geographic CRS (section 2.2) and from GLC_FCS30D data that were reprojected to the UTM projected CRS (section 2.1). These areas in Table 2 are given for 2015 and 2020, along with changes in built-up area and corresponding percentages. Percentages express built-up area change relative to the built-up area in 2015.

When comparing percentages of built-up area changes calculated from data georeferenced in geographic CRS, and in projected one, the largest difference is 0.03% for the Nabatieh governorate. For all other governorates, there is either no difference or the difference is 0.01%, which can partly be attributed to the rounding-related issues. When comparing built-up areas for each year calculated from data in different CRSs, differences go up to 0.05 km^2 (Akkar and Mount Lebanon Governorates).

4 Discussion

From the results listed in Table 2, it can be concluded that when a change in the built-up area has to be calculated, reprojecting data georeferenced in WGS 84 CRS to UTM CRS does not introduce significant differences from changes directly calculated from the data in WGS 84. Although this difference is not significant, traditionally common reprojection step is, as we have shown, obsolete, since modern GIS applications provide a way to make calculations from data georeferenced in geographic CRS. All geospatial raster data have some level of uncertainty associated with them and reprojecting them further increases those uncertainties. Therefore, reprojecting should, if possible, be avoided.

On the other hand, when comparing areas (not changes) in Table 2 that are calculated from data in WGS 84 and in UTM CRS, larger differences can be observed. It is interesting to notice that for both years differences in areas calculated

Table 2. Areas of built-up land cover class calculated from data in different CRSs for 2015 and 2020 and their change for the 10-km coastal zone of Lebanon.

Governorate (area in 10–km CZ)	**Built–up area (km^2)**			
	CRS	**2015**	**2020**	**Change***
Akkar (207.04 km2)	WGS 84	32.22	36.49	4.27 (13.25%)
	UTM	32.27	36.54	4.28 (13.25%)
	Difference (abs.)	0.05	0.05	0.01 (0.00%)
North (450.65 km2)	WGS 84	70.10	71.74	1.64 (2.33%)
	UTM	70.10	71.74	1.64 (2.34%)
	Difference (abs.)	0.00	0.00	0.00 (0.01%)
Keserwan–Jbeil (305.99 km2)	WGS 84	46.94	46.47	–0.47 (–0.99%)
	UTM	46.98	46.52	–0.47 (–1.00%)
	Difference (abs.)	0.04	0.05	0.00 (0.01%)
Beirut (21.47 km2)	WGS 84	17.11	17.03	–0.08 (–0.47%)
	UTM	17.10	17.02	–0.08 (–0.46%)
	Difference (abs.)	0.01	0.01	0.00 (0.01%)
Mount Lebanon (492.97 km2)	WGS 84	115.24	114.91	–0.33 (–0.29%)
	UTM	115.28	114.94	–0.34 (–0.28%)
	Difference (abs.)	0.04	0.03	0.01 (0.01%)
South (582.70 km2)	WGS 84	83.58	85.73	2.15 (2.56%)
	UTM	83.62	85.76	2.14 (2.57%)
	Difference (abs.)	0.04	0.03	0.01 (0.01%)
Nabatieh (35.21 km2)	WGS 84	3.33	3.53	0.20 (6.02%)
	UTM	3.34	3.54	0.20 (6.05%)
	Difference (abs.)	0.01	0.01	0.00 (0.03%)

* change is calculated as: (area in 2020) – (area in 2015); percentages as: [(area in 2020) – (area in 2015)] / (area in 2015)

from data in UTM and in WGS 84 are larger than corresponding differences built-up area change. This means that approximately the same level of difference was introduced in areal calculations for each year, but differences were almost nullified when calculating the change. Although we do not find observed differences to be significant, it must be emphasized that the presented analysis was limited to a relatively small geographical area. If the analysis was performed globally, the calculation procedure would either be notably more complex, or differences would be much larger. Previously stated issues related to georeferencing LCLU data in geographic or projected CRS can be mitigated by georeferencing them with DGGS. By referencing global LCLU products in equal-area DGGS, the process of calculating the area of each LCLU class would be as simple as calculating it from raster data in equal-area projection, while keeping data georeferenced directly on the surface of the ellipsoid. LCLU data production workflow can also benefit from DGGS since it is particularly suitable for 'vertically' integrating data that are linked to a specific location (Li and Stefanakis 2020). This means that all input data that are used for generating LCLU data can first be converted to DGGS and then classification can be performed. However, it should be noted that there are still various issues related to the implementation and acceptance of DGGSs by the GIS community. As Goodchild (2019) states, DGGS is computationally more demanding than current flattened data models and it is conceptually more complex than rasters. From the LCLU data perspective, one issue is the fact that cell size in DGGSs is predetermined by a specific DGGS implementation. This means that DGGS cell size might not match the pixel size of satellite images from which land cover data were extracted.

5 Conclusions

In this paper, we compared two methods of calculating the area of built-up land cover change from LCLU data delivered in raster format. The same raster datasource was used in both methods, but in one method raster was georeferenced in geographic CRS, and in another it was transformed to the projected CRS before calculations. Because of the relatively small geographical scope of the analysis (Lebanese 10-km CZ), no significant differences were observed. However, we showed that it is quite easy to make calculations directly from data in geographic CRS, which is a traditionally avoided approach. We also discussed the benefits of using DGGS in relation to representing LCLU data, especially global ones. One of the main reasons for the potential of the DGGS becoming more widely used is the fact that it represents geographic reality in a way that is more adapted to the actual shape of the Earth, as compared to the current flattened approaches.

Acknowledgments: This research is partially supported through project KK.01.1.1.02.0027, a project co-financed by the Croatian Government and the European Union through the European Regional Development Fund - the Competitiveness and Cohesion Operational Programme.

6 References

Brown, C.F., Brumby, S.P., Guzder-Williams, B., ... Tait, A.M., 2022. Dynamic World, Near real-time global 10 m land use land cover mapping. Scientific Data 9, 251.

[DGIWG] Defence Geospatial Information Working Group, 2020. DGIWG 250 Defence Gridded Elevation Data Product Implementation Profile.

Goodchild, M.F., 2019. Preface. Cartographica 54, 1-3.

Karra, K., Kontgis, C., Statman-Weil, Z., ... Brumby, S.P., 2021. Global land use / land cover with Sentinel 2 and deep learning, in: 2021 IEEE International Geoscience and Remote Sensing Symposium IGARSS. 4704-4707.

Kmoch, A., Matsibora, O., Vasilyev, I., Uuemaa, E., 2022. Applied open-source Discrete Global Grid Systems. AGILE: GIScience Series 3, 1-6.

Lapaine, Miljenko, Lapaine, Miroslava, 1991. Površina elipsoidnog trapeza. Geodetski list 45 (68), 367-373.

Li, M., Stefanakis, E., 2020. Geospatial Operations of Discrete Global Grid Systems—a Comparison with Traditional GIS. Journal of Geovisualization and Spatial Analysis 4, 26.

Lu, M., Appel, M., Pebesma, E., 2018. Multidimensional arrays for analysing geoscientific data. ISPRS International Journal of Geo-Information 7.

Moreira de Sousa, L., Poggio, L., Kempen, B., 2019. Comparison of FOSS4G Supported Equal-Area Projections Using Discrete Distortion Indicatrices. ISPRS International Journal of Geo-Information 8, 351.

Potapov, P., Hansen, M.C., Pickens, A., ... Kommareddy, A., 2022. The Global 2000-2020 Land Cover and Land Use Change Dataset Derived From the Landsat Archive: First Results. Front. Remote Sensing 3, 856903.

Steinwand, D.R., Hutchinson, J.A., Snyder, J.P., 1995. Map projections for global and continental data sets and an analysis of pixel distortion caused by reprojection. Photogramm. Engineering and Remote Sensing 61, 1487-1497.

Zanaga, D., Van De Kerchove, R., De Keersmaecker, W., ... Arino, O., 2021. ESA WorldCover 10 m 2020 v100.

Zhang, X., Zhao, T., Xu, H., Liu, W., ... Liu, L., 2024. GLC_FCS30D: the first global 30 m land-cover dynamics monitoring product with a fine classification system for the period from 1985 to 2022 generated using dense-time-series Landsat imagery and the continuous change-detection method. Earth System Science Data 16, 1353-1381.